Check for updates

CHEMISTRY
A European Journal

A Journal of
ChemPubSoc Europe

Accepted Article

Title: Synthesis and Catalytic Applications of Multi-Walled Carbon Nanotube-Polyamidoamine Dendrimer Hybrids

Authors: Antonin Desmecht, Timothy Steenhaut, Florence Pennetreau, Sophie Hermans, and Olivier Riant

This manuscript has been accepted after peer review and appears as an Accepted Article online prior to editing, proofing, and formal publication of the final Version of Record (VoR). This work is currently citable by using the Digital Object Identifier (DOI) given below. The VoR will be published online in Early View as soon as possible and may be different to this Accepted Article as a result of editing. Readers should obtain the VoR from the journal website shown below when it is published to ensure accuracy of information. The authors are responsible for the content of this Accepted Article.

To be cited as: *Chem. Eur. J.* 10.1002/chem.201802301

Link to VoR: http://dx.doi.org/10.1002/chem.201802301

Supported by
ACES

WILEY-VCH

10.1002/chem.201802301

WILEY-VCH

FULL PAPER

Synthesis and Catalytic Applications of Multi-Walled Carbon Nanotube-Polyamidoamine Dendrimer Hybrids

Antonin Desmecht, Timothy Steenhaut, Florence Pennetreau, Sophie Hermans* and Olivier Riant*[a]

We dedicate this work to the memory of Pr. István E. Markó (1956-2017).

Abstract: Polyamidoamine (PAMAM) dendrimers were covalently immobilized on multi-walled carbon nanotubes (MWNT) *via* two 'grafting to' strategies. We demonstrate the existence of non-covalent interactions between the two components but outline the superiority of our two grafting approaches, namely xanthate and click chemistry. MWNT surfaces were functionalized with activated ester and propargylic moieties prior to their reaction with PAMAM or azido-PAMAM dendrimers, respectively. The grafting of PAMAM generations 0 to 3 was evaluated with X-ray photoelectron spectroscopy (XPS), thermogravimetric analysis (TGA) and transmission electron microscopy (TEM). The versatility of our hybrids was demonstrated by post-functionalization sequences involving copper alkyne-azide cycloaddition (CuAAC). We synthesized homogeneous supported iridium complexes at the extremities of the dendrimers. In addition, our materials were used as template for the encapsulation of Pd nanoparticles (NP), validating our nanocomposites for catalytic applications. The palladium-based catalyst was active for carbonylative coupling during 5 consecutive runs without loss of activity.

Introduction

Throughout the last decades, nanocarbon-based hybrids piqued scientific community's curiosity.[1–7] This interest can easily be explained by the fact that each component of the material is able to bring up peculiar properties and, together, form a composite with a combination of unique functionalities. By extension, composites can even exhibit new properties resulting from the synergy of their constituents. In this context, nanohybrids composed of nanocarbons (NCs) and dendrimeric structures have proven to be of great interest.[8–21] NCs such as single-/multi-walled carbon nanotubes (S-/MWNTs) and graphene (G) have very high physical and chemical stabilities, exceptional thermic and electric conductivities and relatively high surface areas. However, NCs are prompt to stack together through π-π stacking. The resulting aggregates show very low solubility or dispersibility in most organic solvents and especially in water. On the opposite, dendrimeric architectures like polyamidoamines (PAMAM) dendrimers display high solubility, reactive peripheral amino groups and unlike most polymers, are accurately defined.[22] These structures offer for instance precise spots for catalytic sites, *i.e.* in the dendrimer core or at its terminations.[23] Those locations are able to host either metallic nanoparticles (NPs) or organometallic complexes for homogeneous-like catalytic applications.[23–29] Dendrimers can also fill in a role of encapsulating vectors in the field of nanomedicine and are intensively studied in drug delivery systems.[26,30–38]

The combination of NCs and PAMAM gives various advantages. First of all, dendrimers significantly increase the dispersibility of the carbonaceous material and therefore favor its handling and processability. Secondly, dendrimers face the usual drawbacks of homogeneous catalytic systems. They are tedious to recover and recycle. This is especially true for small size dendrimers. However, once grafted on NCs, dendrimeric systems are easily separable from the medium and can therefore be recovered and used again. Thirdly, the use of carbon nanotubes (CNTs) in nanomedicine is still discussed as their toxicity is yet to be fully understood. It is commonly accepted that pristine CNTs (p-CNTs) are cytotoxic and cause inflammation to human organs. However, the modification of nanotubes surfaces alters their behavior towards biological systems and reduces their toxicity.[39–41] Grafting dendrimers on CNTs surfaces enables such phenomenon.[33,34] In addition, dendrimer's anchoring is highly valuable as the amount of surface reactive sites is therefore considerably augmented depending on the size of the dendrimer.

Numerous examples of nanohybrids CNT-PAMAM have already been studied but few propose a systematic study of functionalization efficiency, especially when comparing covalent with non-covalent approaches. Two main strategies are commonly used for the immobilization of dendrimers on CNTs, namely the 'grafting from' and 'grafting to' approaches. In the first case, the dendrimers are grown sequentially *in situ* on the surface.[14,34,42–56] The main drawback of this methodology is that the conversion at each step of dendrimer growth is not complete and therefore a mixture of dendrimers is present on the final surface. In the latter case, a fully grown dendrimeric structure is attached directly on the nanotube.[57–65] In most cases, this immobilization is achieved through amidation reactions between carboxylic acid groups on the carbonaceous surface and the amino groups of the PAMAM. However, an oxidative pre-treatment of the support is needed to increase the number of such carboxylic functions. This preliminary step often results in the shortening or the collapsing of CNTs, together with introduction of many defect sites, inducing therefore a partial or complete loss of electric conductivity that is essential in many applications. In addition, carboxylic groups are thermally-sensitive functions,

[a] A. Desmecht, T. Steenhaut, Dr. F. Pennetreau, Prof. S. Hermans, Prof. O. Riant
Institute of Condensed Matter and Nanosciences, Molecules, Solids and Reactivity (IMCN/MOST)
Université catholique de Louvain
Place Louis Pasteur 1, 1348 Louvain-la-Neuve (Belgium)
E-mail: olivier.riant@uclouvain.be
sophie.hermans@uclouvain.be
Supporting information for this article is given via a link at the end of the document.

Accepted Manuscript

This article is protected by copyright. All rights reserved.

10.1002/chem.201802301

easily removed upon heating. Although Prato *et al.* reported another strategy using disulfides for the radical grafting of dendrimers,[63] alternatives to amidation are still scarce in the literature. In addition to covalent immobilization, dendrimers can also be adsorbed on NC in a non-covalent fashion.[66–70] Non-covalent interactions are known to occur through ionic interplays between the positively charged terminal amines of the dendrimer and the negatively charged carboxylates from the support. Moreover the macromolecule wrap around nanotubes via hydrophobic, π−π or CH−π interactions.

We propose hereby the study of covalent grafting of ethylenediamine core PAMAM dendrimers on CNTs by the means of two different 'grafting to' approaches and systematic comparison with non-covalent immobilization. The grafted macromolecules will prove their utility as they significantly increase the number of active sites per nanotube. Their primary amino groups will be derivatized into azido moieties to undergo CuAAC click reaction leading to triazole-functionalized terminations. Although this transformation is well-known in organic synthesis, Jacobson *et al.* were the only ones to our knowledge to report this transformation on unsupported PAMAM dendrimers.[71,72] We could successfully immobilize a significant amount of metal thanks to the dendrimers and the resulting composites were evaluated for catalytic applications in both homogeneous supported (*i.e.* organometallic complexes) and heterogeneous (*i.e.* metallic nanoparticles) catalysis.

Results and Discussion

We reported in 2013 the covalent functionalization of nanocarbons with xanthates using peroxides as radical initiators.[73,74] Following this procedure, we were able to graft an activated ester on *p*-MWNT and the fluorine content of the resulting material **1** was evaluated by XPS to be 2.28 at.%. More recently, we reported the efficient grafting of propargylic moieties on NC surface and emphasized their use as precursors for CuAAC post-functionalization.[75] Support **2** was synthesized according to this procedure (Scheme 1A).

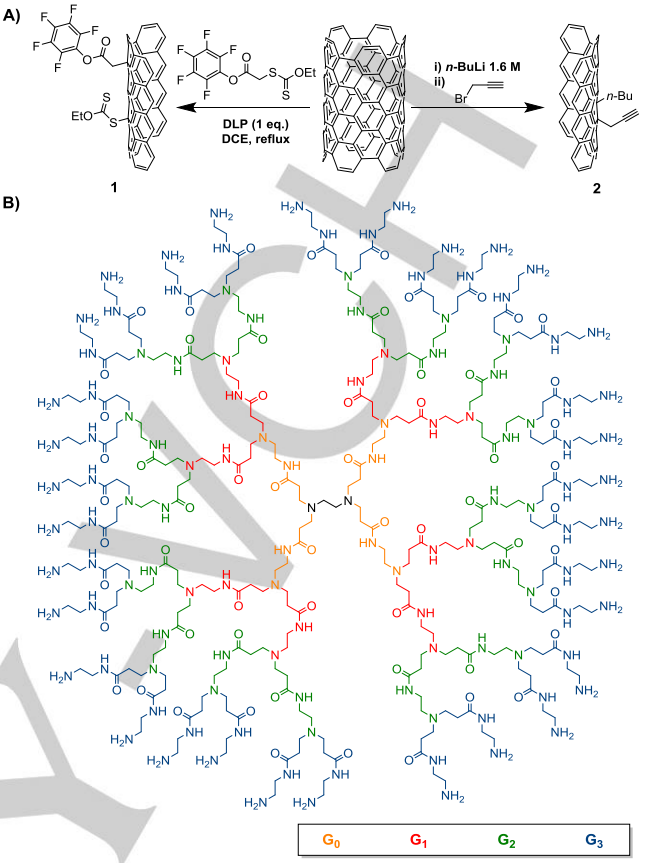

Scheme 1. A) Covalent functionalization of MWNTs with xanthate (left) or propargylic (right) moieties, B) PAMAM dendrimers of generation 0 to 3.

Commercial PAMAM dendrimers (20 wt.% in methanol) of different generations (0 to 3) were used in this work (Scheme 1B). The primary amines were able to react with the activated esters of **1**, leading to the formation of an amide bond and the materials **3-G$_{0-3}$** as an homogeneous black suspension (Scheme 2A). Products **3-G$_{0-3}$** were characterized by the means of X-ray photoelectron spectroscopy (XPS) and thermogravimetric analysis (TGA). XPS shows a significant decrease in fluorine content after dendrimer grafting, going from 2.28 at.% to 0.84 at.% (Figure 1A) which indicates the effective reaction between **1** and dendrimers. The amount of nitrogen increases with the dendrimer generation (Table 1).

Accepted Manuscript

This article is protected by copyright. All rights reserved.

10.1002/chem.201802301

FULL PAPER

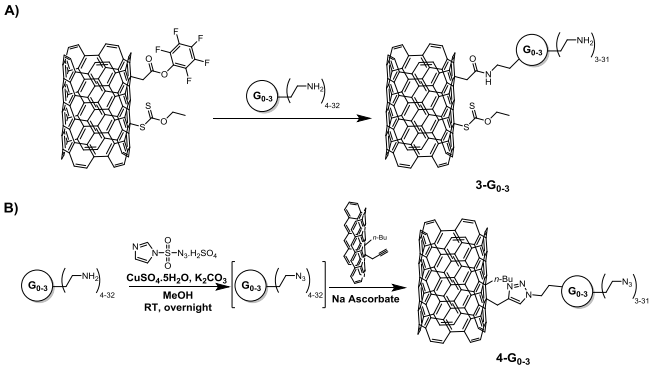

Scheme 2. Grafting of generation 0-3 PAMAM dendrimers on A) xanthate or B) propargylic functionalized MWNTs.

Table 1. XPS analysis of **3-G$_{0-3}$**, **4-G$_{0-3}$** and **5-G$_{0-3}$** (at.%).

	3-G$_{0-3}$			**4-G$_{0-3}$**			**5-G$_{0-3}$**		
Gen	C_{1s}	O_{1s}	N_{1s}	C_{1s}	O_{1s}	N_{1s}	C_{1s}	O_{1s}	N_{1s}
0	94.37	3.17	1.26	92.62	4.78	2.60	96.96	1.86	1.19
1	93.24	3.14	2.35	88.85	6.43	4.72	95.74	2.55	1.71
2	90.38	5.26	3.21	87.58	6.05	6.37	92.73	3.76	3.51
3	87.85	6.92	3.68	81.57	7.30	11.13	90.56	4.87	4.57

Prior to their reaction with chemical platform **2**, dendrimers were turned into azido-PAMAM thanks to the imidazole-1-sulfonyl azide sulfuric acid salt (Scheme 2B).[76] The resulting azido-PAMAM were not isolated and directly contacted in solution with **2**. The azide synthesis is catalyzed by a copper (II) species whereas CuAAC is catalyzed by a copper (I) species. Therefore, sodium ascorbate was added at the same time in order to reduce Cu(II) into Cu(I). This strategy enables the direct transformation of primary amines into triazole click products in a one-pot process in a similar way to the one described by Stonehouse *et al.* in 2009.[77] Azido PAMAM and **2** were reacted in suspension for a very short time to avoid the grafting of the dendrimer through multiple extremities leading to a multipodal composite. Azido hybrids **4-G$_{0-3}$** were investigated by XPS and TGA as well. The XPS spectrum of **4-G$_{0-3}$** in the N_{1s} region revealed the presence of remaining azide moieties at 405 eV (Figure 1B). Again, the nitrogen content increases with the size of PAMAM dendrimer (Table 1).

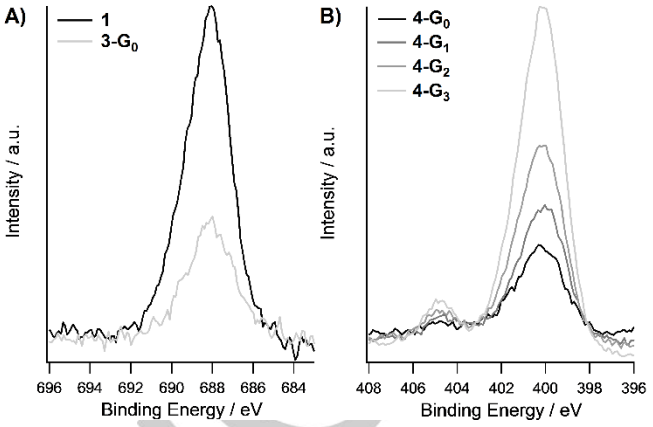

Figure 1. XPS spectra of A) F_{1s} region (xanthate strategy) and B) N_{1s} region (click strategy).

Beside the covalent immobilization of those macromolecules on our supports, non-covalent interactions were also considered and blank experiments were carried out. Those control experiments were run by incubation of nanotubes with PAMAM dendrimers in the same conditions as above. *p*-MWNTs were incubated with generation 0-3 PAMAM dendrimers, leading to the hybrids **5-G$_{0-3}$**. The resulting composites were carefully and repeatedly washed before analysis to make sure that PAMAM dendrimers are strongly immobilized on nanotubes. Those compounds were studied by XPS and TGA (Table 1). The quantity of nitrogen was determined and compared for all those samples by the means of XPS. For the comparison to be reliable, one should carefully pay attention to the specific amount of nitrogen in the hybrids. **3-G$_{0-3}$** and **5-G$_{0-3}$** can be compared one by one easily as each generation of dendrimer has the same number of N. However, **4-G$_{0-3}$** has three N atoms on each extremity whereas **3-G$_{0-3}$** and **5-G$_{0-3}$** have only one. Therefore, the quantity of N presented in Table 1 was normalized according to the relative abundance of nitrogen on the extremities of the dendrimers (Figure 2). More detail on the calculations can be found in the supporting information. The increase of nitrogen contents can be observed for each series of hybrids. Whereas N content is very similar for series **3-G$_{0-3}$** and **5-G$_{0-3}$**, one can clearly see that samples **4-G$_{0-3}$** have the highest nitrogen content values, which indicates a more efficient immobilization of PAMAM on MWNTs. In order to have a better insight on our methodologies, TGA was used as a complementary analytical tool. When hybrids of generation 0 (**3-G$_0$**, **4-G$_0$** and **5-G$_0$**) are compared, a lower amount of immobilized dendrimer is observed for non-covalent interactions (6.7 wt.%). However, we notice an identical loading of 11.4 wt.% for **3-G$_0$** and **4-G$_0$** (Figure 3A). This trend is confirmed by TGA of generation 3 hybrids (**3-G$_3$**, **4-G$_3$** and **5-G$_3$**) (Figure 3B). Non-covalent stacking leads to 18.0 wt.% whereas covalent binding enables the grafting of roughly 30 wt.%. We can therefore conclude that the covalent strategies significantly increase the amount of dendrimers which can be immobilized on MWNTs. A significant difference of loading is observed by XPS analysis while the loading seems identical using TGA for **3-G$_{0,3}$** and **4-G$_{0,3}$**. This difference can be rationalized simply by the fact that XPS is a surface analysis

Accepted Manuscript

This article is protected by copyright. All rights reserved.

10.1002/chem.201802301

technique and that the increasing thickness of the polymer layer on the hybrids surface is such that XPS is not able to probe the whole layer anymore. Loading determination by means of TGA shall hence be favored. Each generation of clicked dendrimers (**4-G_{0-3}**) were submitted to TGA as well. We observe regular loading increase as the dendrimer expands (Figure 3C).

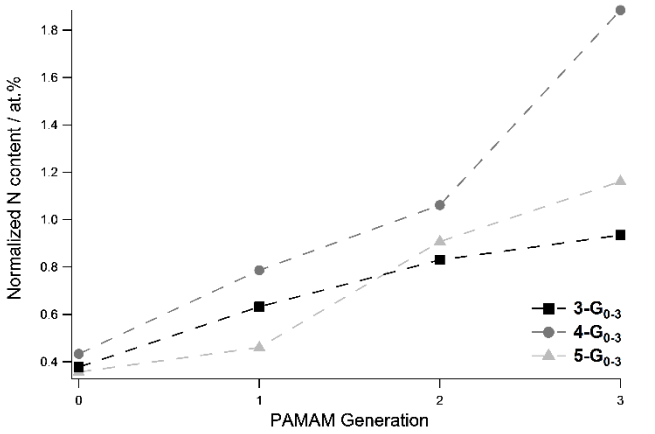

Figure 2. XPS data comparison of the hybrids obtained by the xanthate, click and non-covalent strategies.

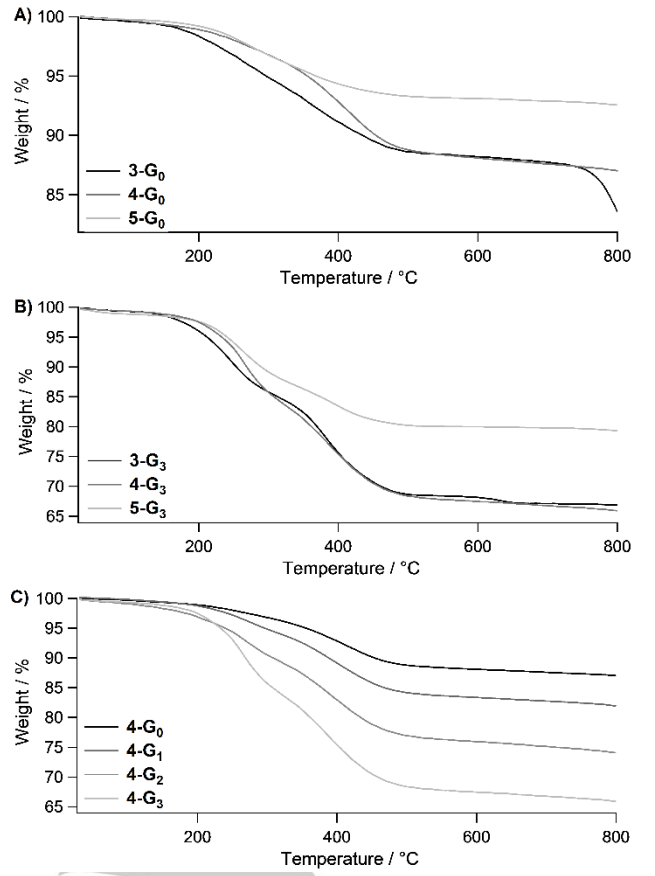

Figure 3. Comparative TGA graphs recorded under N_2 atmosphere: A) generation 0, B) generation 3 and C) generation 0-3 from click strategy. Mass losses correspond to functionalization degree.

Going a step further, we exploited the presence of polyamidoamines on our supports for post-functionalization through click chemistry. The amino extremities of **3-G_0** were turned into azides with imidazole-1-sulfonyl azide sulfuric acid salt as described previously to give compound **6-G_0** (Scheme 3A). Those azides were brought in presence of 4-chlorophenylacetylene, copper iodide and *N,N,N',N'',N''*-pentamethyldiethylenetriamine (PMDETA) to yield triazoles **7-G_0**. XPS analysis of **7-G_0** indicates the presence of 0.28 at.% of chlorine. A closer look at Cl/N ratios obtained by XPS indicates the conversion of all free extremities of the generation 0 dendrimer into triazoles. In fact, we observe a small excess of chlorine compared to nitrogen which could result from the adsorption of the acetylene derivative on the nanotube C_{sp2} surface through π-π stacking. We also reacted the remaining azide functions of **4-G_{0-3}** with 3-trifluoromethylphenyl acetylene, CuI and PMDETA to yield **8-G_{0-3}**. Their XPS analysis revealed fluorine that increased with dendrimer's generation, as clearly seen on Figure 4. The comparison of the experimental N/F ratio with the theoretical one (2 for each generation) suggests that all the free extremities of each dendrimer generation are transformed into clicked products. In the case of **8-G_3**, the N/F ratio is lower than expected which can be explained by the adsorption or the trapping of phenylacetylene on nanotube or inside dendrimers. Those transformations outlined the utility of grafting dendrimers on carbon nanotubes as we dramatically increased the quantity of functions that can be grafted on MWNTs surfaces by the conventional methods. Although the F/C ratios can reach up to 0.51 for direct fluorination of SWNTs,[78] the F/C ratio of fluorophenyl-functionalized SWNTs obtained from aryl diazonium salts do not exceed 0.037.[79] The F/C ratio of **8-G_3** could be as high as 0.082 (3 F atoms per function) which is considerably high taking into account the fact that the support is MWNT (higher C content) and not SWNT. For comparison, the F/C ratio value of **1** is 0.024 (5 F atoms per function).

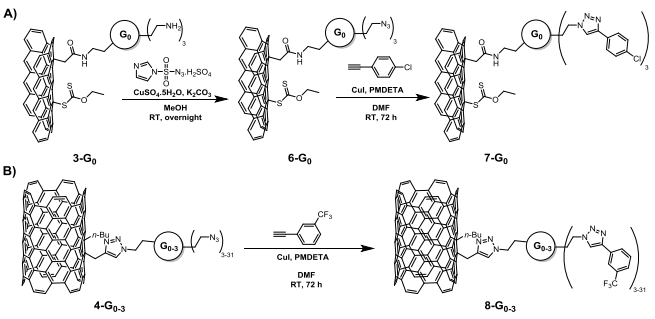

Scheme 3. Post-functionalization of PAMAM hybrids into triazole adducts.

Accepted Manuscript

This article is protected by copyright. All rights reserved.

10.1002/chem.201802301

Table 2. XPS analysis of post-functionalized dendrimers **8-G$_{0-3}$** (at.%).

Gen	C_{1s}	O_{1s}	N_{1s}	F_{1s}	N/F
0	91.53	4.68	2.66	1.13	2.35
1	88.10	5.58	4.18	2.14	1.95
2	83.57	7.25	6.05	3.14	1.93
3	77.19	6.79	9.67	6.35	1.52

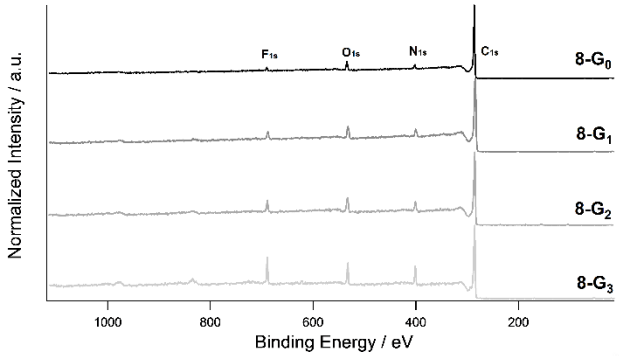

Figure 4. General XPS survey of hybrids **8-G$_{0-3}$**.

p-MWNTs, hybrids **3-G$_3$** and **4-G$_3$** were also characterized by transmission electron microscopy (TEM). No significant difference was observed between pristine nanotubes and composite **3-G$_3$** (Figure 5A,B). However, one can observe the formation of an external layer of dendrimers on hybrid **4-G$_3$** (Figure 5C,D). This external layer has a thickness of approximatively 8 to 10 nm and seems to be present as randomly dispersed patches on nanotubes. This surface structure difference between **3-G$_3$** and **4-G$_3$** is supported by the differences observed in the XPS measurements of **3-G$_3$** and **4-G$_3$**, whereas the TGA measurements do not show significant variations.

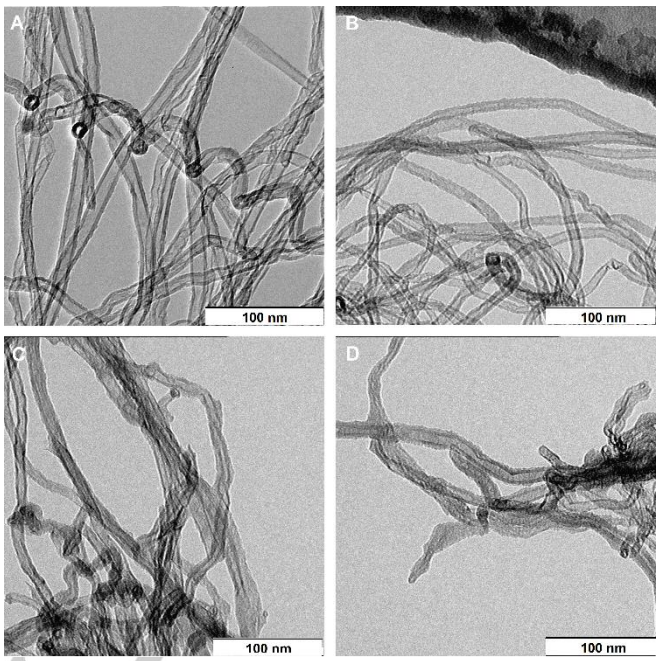

Figure 5. TEM images of A) *p*-MWNTs, B) **3-G$_3$**, C and D) **4-G$_3$**.

We further demonstrated the utility of our grafted materials through the synthesis of two composites with catalytic activity exploiting the presence of PAMAM dendrimers on carbon nanotubes. Starting from **4-G$_3$**, we clicked 2-ethynyl-4-methoxypyridine in the presence of CuI and PMDETA to afford **9-G$_3$** (Scheme 4A). The formation of the triazole-pyridine moiety enables the use of such composite as bidentate ligand, for the complexation of various metallic centres.[80–82] The use of the dimer $[IrCp^*Cl_2]_2$ as precursor leads to supported iridium complexes **10-G$_3$**. This composite was characterized by XPS and inductively coupled plasma atomic emission spectroscopy (ICP-AES). It is noteworthy that for the sake of dendrimer economy, 0.2 equivalents of PAMAM were employed for the synthesis of **4-G$_3$** instead of 2 equivalents as described above. Although the amount of introduced dendrimer is 10 times less important, we observe a nitrogen content of 7.03 at.% which is only 27 % lower and really appreciable (Table 3). The XPS analysis of **10-G$_3$** revealed the presence of 0.79 at.% of Ir (Figure 6A) whereas bulk ICP-AES indicates a content in Ir of 7.71 wt.%. Looking at the structure of the functionalized dendrimer, 124 out of 217 N atoms (57 %) come from the triazole-pyridine ligand which means that 3.69 at.% N are dedicated to Ir complexation. This amount can be divided by 4 as 4 atoms of N are present for 1 atom of Ir. We can therefore conclude that the theoretical maximum loading of Ir would be 0.92 at.%. We were pleased to see the matching between the calculated and the experimental value of 0.79 at.% which means that our strategy and the reactions involved are reliable and efficient. As a proof of concept, a preliminary experiment with the iridium-based composite was carried out for catalytic reduction reactions. **10-G$_3$** could successfully reduce an imine into the corresponding amine in presence of sodium formate as hydride source with 31 % conversion after 4 hours at 80 °C (Scheme 4B).

Accepted Manuscript

This article is protected by copyright. All rights reserved.

10.1002/chem.201802301

This preliminary experiment remains to be optimized but shows the possibility of high loading of metal complexes on CNTs for potential applications in organometallic catalysis.

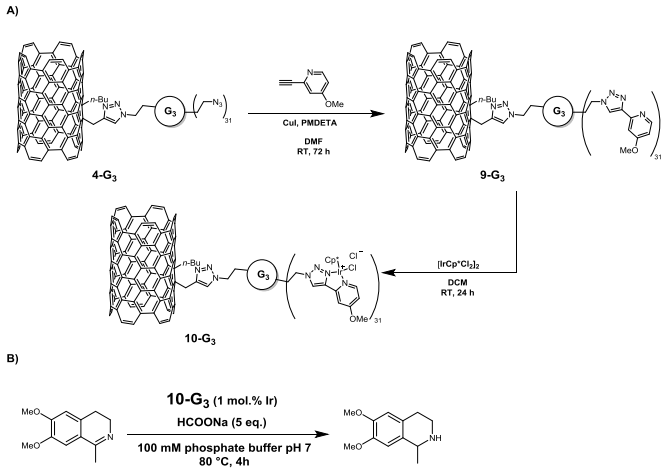

Scheme 4. A) Synthesis of bidentate supported ligand **9-G$_3$** and supported Ir complex **10-G$_3$** and B) its catalytic application for imine reduction.

Table 3. XPS analysis of post-functionalized dendrimers (at.%).

Gen	C_{1s}	O_{1s}	N_{1s}	Ir_{4f}	Cl_{2p}	Pd_{3d}
9-G$_3$	86.10	6.82	7.03	-	-	-
10-G$_3$	84.85	6.58	6.46	0.79	1.68	-
11-G$_1$	91.23	5.99	2.64	-	-	-
12-G$_1$	88.43	7.84	2.47	-	-	1.25

In addition to the post-functionalization of the PAMAM extremities, we also demonstrated the ability of the supported dendrimers to host nanoparticles. The azido moieties of **4-G$_1$** were reduced into amines using the Staudinger reaction to give nanocomposite **11-G$_1$** in order to favour the interactions between free extremities and metallic precursors (Scheme 5A). As described previously, the quantity of introduced PAMAM was reduced from 2 to 0.2 eq. The quantity of immobilized dendrimer was here (for G_1 generation) only reduced by 19 % according to TGA analysis. The disappearance of N azido component on the XPS spectrum at 405 eV was noticed for **11-G$_1$** (Figure 6B). The N content was reduced from 3.94 at.% to 2.64 at.% which is in agreement with the loss of 2 N atoms per extremity. An aqueous solution of Na_2PdCl_4 was stirred with a suspension of **11-G$_1$** and the resulting mixture was filtered, washed and finally reduced with a solution of sodium borohydride to yield **12-G$_1$**. Compound **12-G$_1$** was investigated by XPS and TGA. XPS spectrum of Pd region revealed 1.25 at.% of Pd in proportions of 65 % of $Pd^{(0)}$ and 35 % of $Pd^{(II)}$ (Figure 6C). The asymmetry of metallic Pd peaks was not taken into account and therefore the amount of Pd(0) is underevaluated. Thermal treatment of **12-G$_1$** in air leads to the formation of 15.5 wt.% of palladium oxide residue. The first weight loss observed on the TGA curve is due to the combustion of dendrimers (Figure 6D).

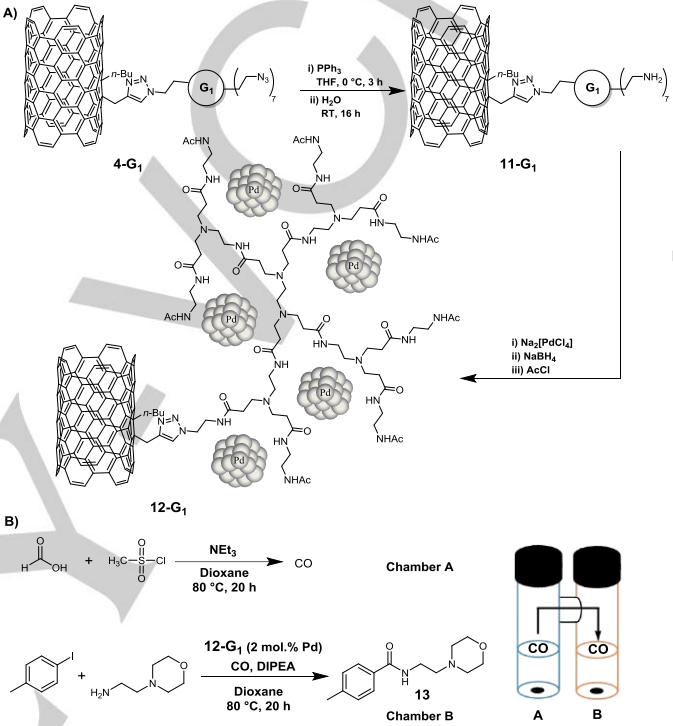

Scheme 5. A) Synthesis of Pd nanoparticles encapsulated in immobilized PAMAM dendrimers on MWNTs and B) their catalytic application for carbonylative coupling.

Accepted Manuscript

This article is protected by copyright. All rights reserved.

10.1002/chem.201802301

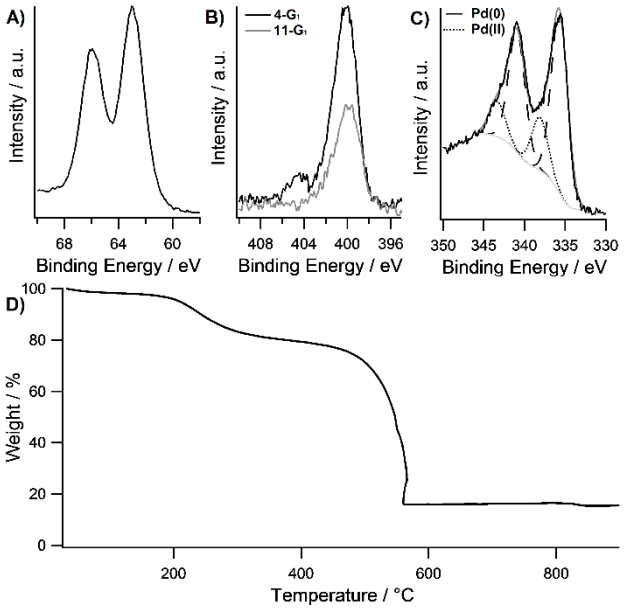

Figure 6. XPS spectra in A) Ir region of **10-G$_3$**, B) N region of **4-G$_1$** and **11-G$_1$**, C) Pd region of **12-G$_1$**, D) TGA graph of **12-G$_1$** recorded under aerobic atmosphere.

We investigated the activity of **12-G$_1$** for carbonylative coupling with *ex situ* generated CO (Scheme 5B). In a double-chamber reactor using the technology developed by the group of Skrydstrup,[83] carbon monoxide is produced by decomposition of formic acid in presence of triethylamine and mesyl chloride according to the procedure described by De Borggraeve *et al*.[84] The use of such device enables the handling of this deadly gas in a safe environment. The generated CO goes up in the second chamber where **12-G$_1$** is in presence of iodotoluene and 4-(2-aminoethyl)morpholine and is consumed to produce the desired amino-carbonylation product **13,** which we obtained with 49 % NMR yield. Residual iodotoluene was also present in the reaction mixture. Our catalyst was recycled by mere filtration and reused 4 times. We observed an increased reactivity after the first run to reach about 80 % conversion after the fifth run (Figure 7). XPS analysis of **12-G$_1$** after the first and the fifth runs indicated the decrease of Pd surface content from 1.25 at.% to 0.36 at.% and then 0.25 at.%. This decrease can be partially explained by the leaching of residual Pd$^{(II)}$ from the catalyst synthesis. However, this leaching had no negative effect on the activity of our composite, quite the opposite.

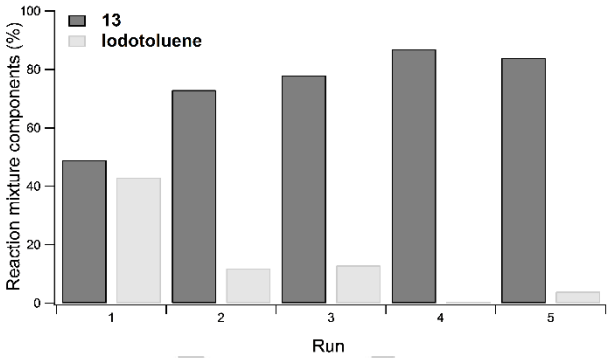

Figure 7. Recycling of **12-G$_1$** in the carbonylative coupling between iodotulene and 4-(2-aminoethyl)morpholine.

A closer look was taken on **12-G$_1$** before catalysis and after the fifth run with TEM. The encapsulating ability of **12-G$_1$** is demonstrated through the preferential immobilization of Pd NPs inside dendrimer layers rather than on nanotubes bare surface (Figure 8A,B). The presence of dendrimers templates the formation of small NPs (2 nm) with a narrow size distribution (see inset). However, the size of Pd NPs increases after catalysis to reach about 6-8 nm (Figure 8C,D). This difference in NPs sizes before and after catalysis explains the difference in Pd content determined with XPS. This variation of size suggests that some catalytic species are leached away during the process due to Pd(0)/Pd(II) mechanism before they redeposit on immobilized NPs, thus increasing their size.

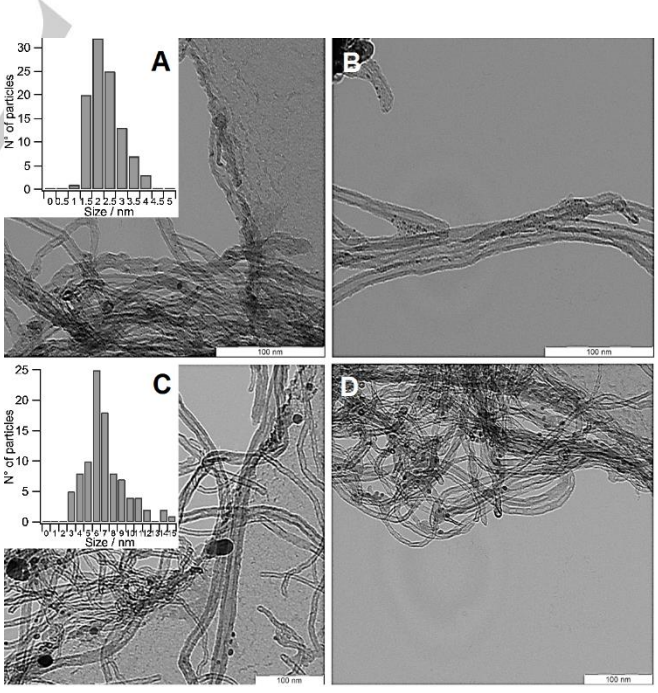

Figure 8. TEM images of **12-G$_1$** before catalysis (A,B) and after the fifth run (C,D).

Accepted Manuscript

This article is protected by copyright. All rights reserved.

Conclusions

To summarize, we presented the immobilization of PAMAM dendrimers on MWNTs by the means of radical and click chemistry. We outlined the existence of non-covalent interactions between dendrimers and support but demonstrated the superiority of covalent functionalization. Hybrid materials were investigated through TGA, XPS and TEM analyses. We propose a convenient PAMAM post-functionalization sequence based on the synthesis of azido dendrimers and subsequent CuAAC reaction with alkynyl derivatives. This process was proven efficient as a high loading of functionalized PAMAM was obtained. The synthesized nanocomposites were exploited either by grafting iridium complexes as supported homogeneous catalysts at the extremities of the dendrimers or by encapsulating palladium nanoparticles within their branches for carbonylative coupling. Our approach enables the use of such hybrids in various applications like catalysis or drug delivery.

Acknowledgements

The authors wish to thank the Fonds de la Recherche Scientifique (F.R.S.-FNRS), the Fonds pour la Formation à la Recherche dans l'Industrie et dans l'Agriculture (FRIA), as well as the Université catholique de Louvain for funding. We are grateful to Jean-François Statsyns and François Billard for technical assistance. We are also thankful to Tommy Haynes for TEM images.

Keywords: carbon nanotubes • PAMAM dendrimer • functionalization • click chemistry • catalysis

[1] D. Eder, *Chem. Rev.* **2010**, *110*, 1348–1385.
[2] C. Sanchez, P. Belleville, M. Popall, L. Nicole, *Chem. Soc. Rev.* **2011**, *40*, 696–753.
[3] S. C. Tjong, *Mater. Sci. Eng. R Reports* **2013**, *74*, 281–350.
[4] G. Yu, X. Xie, L. Pan, Z. Bao, Y. Cui, *Nano Energy* **2013**, *2*, 213–234.
[5] Y. Liang, Y. Li, H. Wang, H. Dai, *J. Am. Chem. Soc.* **2013**, *135*, 2013–2036.
[6] P. T. Yin, S. Shah, M. Chhowalla, K. B. Lee, *Chem. Rev.* **2015**, *115*, 2483–2531.
[7] N. K. Mehra, N. K. Jain, *J. Drug Target.* **2016**, *24*, 294–308.
[8] Y. P. Sun, W. Huang, Y. Lin, K. Fu, A. Kitaygorodskiy, L. A. Riddle, Y. J. Yu, D. L. Carroll, *Chem. Mater.* **2001**, *13*, 2864–2869.
[9] M. Holzinger, J. Abraham, P. Whelan, R. Graupner, L. Ley, F. Hennrich, M. Kappes, A. Hirsch, *J. Am. Chem. Soc.* **2003**, *125*, 8566–8580.
[10] E. Murugan, S. Arumugam, P. Panneerselvam, *Int. J. Polym. Mater. Polym. Biomater.* **2016**, *65*, 111–124.
[11] A. Masotti, M. R. Miller, A. Celluzzi, L. Rose, F. Micciulla, P. W. F. Hadoke, S. Bellucci, A. Caporali, *Nanomedicine Nanotechnology, Biol. Med.* **2016**, *12*, 1511–1522.
[12] J. P. C. Trigueiro, R. C. Figueiredo, J. Rojo, R. M. R. Viana, M. C. Schnitzler, G. G. Silva, *J. Solid State Electrochem.* **2016**, *20*, 1991–2000.
[13] S. J. Tabatabaei Rezaei, H. Khorramabadi, A. Hesami, A. Ramazani, V. Amani, R. Ahmadi, *Ind. Eng. Chem. Res.* **2017**, *56*, 12256–12266.
[14] S. Campidelli, C. Sooambar, E. L. Diz, C. Ehli, D. M. Guldi, M. Prato, *J. Am. Chem. Soc.* **2006**, *128*, 12544–12552.
[15] A. García, M. A. Herrero, S. Frein, R. Deschenaux, R. Muñoz, I. Bustero, F. Toma, M. Prato, *Phys. Status Solidi Appl. Mater. Sci.* **2008**, *205*, 1402–1407.
[16] T. Palacin, H. Le Khanh, B. Jousselme, P. Jegou, A. Filoramo, C. Ehli, D. M. Guldi, S. Campidelli, *J. Am. Chem. Soc.* **2009**, *131*, 15394–15402.
[17] J. McCarroll, H. Baigude, C. S. Yang, T. M. Rana, *Bioconjug. Chem.* **2010**, *21*, 56–63.
[18] J.-T. Sun, C.-Y. Hong, C.-Y. Pan, *Polym. Chem.* **2011**, *2*, 998.
[19] E. Murugan, G. Vimala, *J. Colloid Interface Sci.* **2013**, *396*, 101–111.
[20] E. Murugan, S. Arumugam, *RSC Adv.* **2014**, *4*, 35428.
[21] R. Soleyman, M. Adeli, *Polym. Chem.* **2015**, *6*, 10–24.
[22] S. M. Grayson, J. M. J. Fréchet, *Chem. Rev.* **2001**, *101*, 3819–3867.
[23] D. Astruc, D. Wang, C. Deraedt, L. Liang, R. Ciganda, J. Ruiz, *Synth.* **2015**, *47*, 2017–2031.
[24] S. M. Lu, H. Alper, *J. Am. Chem. Soc.* **2005**, *127*, 14776–14784.
[25] A. Mansour, T. Kehat, M. Portnoy, *Org. Biomol. Chem.* **2008**, *6*, 3382–7.
[26] D. Astruc, E. Boisselier, C. Ornelas, *Chem. Rev.* **2010**, *110*, 1857–1959.
[27] P. Govender, T. Riedel, P. J. Dyson, G. S. Smith, *J. Organomet. Chem.* **2015**, *799–800*, 38–44.
[28] P. Neumann, H. Dib, A. Sournia-Saquet, T. Grell, M. Handke, A. M. Caminade, E. Hey-Hawkins, *Chem. - A Eur. J.* **2015**, *21*, 6590–6604.
[29] A. M. Caminade, A. Ouali, R. Laurent, C. O. Turrin, J. P. Majoral, *Coord. Chem. Rev.* **2016**, *308*, 478–497.
[30] R. Esfand, D. A. Tomalia, *Drug Discov. Today* **2001**, *6*, 427–436.
[31] S. Svenson, D. A. Tomalia, *Adv. Drug Deliv. Rev.* **2005**, *57*, 2106–2129.
[32] S. Svenson, *Eur. J. Pharm. Biopharm.* **2009**, *71*, 445–462.
[33] X. Shi, S. H. Wang, M. Shen, M. E. Antwerp, X. Chen, C. Li, E. J. Petersen, Q. Huang, W. J. Weber, J. R. Baker, *Biomacromolecules* **2009**, *10*, 1744–1750.
[34] B. Pan, D. Cui, P. Xu, C. Ozkan, G. Feng, M. Ozkan, T. Huang, B. Chu, Q. Li, R. He, et al., *Nanotechnology* **2009**, *20*, 125101–125109.
[35] S. Parveen, R. Misra, S. K. Sahoo, *Nanomedicine Nanotechnology, Biol. Med.* **2012**, *8*, 147–166.
[36] R. M. Kannan, E. Nance, S. Kannan, D. A. Tomalia, *J.*

Accepted Manuscript

This article is protected by copyright. All rights reserved.

Intern. Med. **2014**, *276*, 579–617.

[37] P. I. Siafaka, N. Üstündağ Okur, E. Karavas, D. N. Bikiaris, *Int. J. Mol. Sci.* **2016**, *17*, DOI 10.3390/ijms17091440.

[38] S. Mignani, J. Rodrigues, H. Tomas, M. Zablocka, X. Shi, A.-M. Caminade, J.-P. Majoral, *Chem. Soc. Rev.* **2018**, DOI 10.1039/C7CS00550D.

[39] R. Soleyman, S. Hirbod, M. Adeli, *Biomater. Sci.* **2015**, *3*, 695–711.

[40] G. Hong, S. Diao, A. L. Antaris, H. Dai, *Chem. Rev.* **2015**, *115*, 10816–10906.

[41] R. Alshehri, A. M. Ilyas, A. Hasan, A. Arnaout, F. Ahmed, A. Memic, *J. Med. Chem.* **2016**, acs.jmedchem.5b01770.

[42] L. Maggini, F. M. Toma, L. Feruglio, J. M. Malicka, T. Da Ros, N. Armaroli, M. Prato, D. Bonifazi, *Chem. - A Eur. J.* **2012**, *18*, 5889–5897.

[43] G. M. Neelgund, A. Oki, Z. Luo, *Colloids Surfaces B Biointerfaces* **2012**, *100*, 215–221.

[44] Y. Zhang, Y. Li, P. Zhang, *J. Mater. Sci.* **2014**, 3469–3477.

[45] A. Herreros-López, C. Hadad, L. Yate, A. A. Alshatwi, N. Vicentini, T. Carofiglio, M. Prato, *European J. Org. Chem.* **2016**, *2016*, 3186–3192.

[46] B. Gao, R. Zhang, F. Gao, M. He, C. Wang, L. Liu, L. Zhao, H. Cui, *Langmuir* **2016**, *32*, 8339–8349.

[47] Y. Fan, G. Wu, F. Su, K. Li, L. Xu, X. Han, Y. Yan, *Fuel* **2016**, *178*, 172–178.

[48] Y. Fan, C. Ke, F. Su, K. Li, Y. Yan, *Energy and Fuels* **2017**, *31*, 4372–4381.

[49] L. Cao, W. Yang, J. Yang, C. Wang, S. Fu, *Chem. Lett.* **2004**, *33*, 490–491.

[50] B. Pan, D. Cui, F. Gao, R. He, *Nanotechnology* **2006**, *17*, 2483–2489.

[51] W. Yuan, G. Jiang, J. Che, X. Qi, R. Xu, M. W. Chang, Y. Chen, S. Y. Lim, J. Dai, M. B. Chan-park, *J. Phys. Chem. B* **2008**, *112*, 18754–18759.

[52] Y.-Z. You, J.-J. Yan, Z.-Q. Yu, M.-M. Cui, C.-Y. Hong, B.-J. Qu, *J. Mater. Chem.* **2009**, *19*, 7656.

[53] J. Che, W. Yuan, G. Jiang, J. Dai, S. Y. Lim, M. B. Chan-park, *Chem. Mater.* **2009**, 1471–1479.

[54] M. A. Herrero, F. M. Toma, K. T. Al-Jamal, K. Kostarelos, A. Bianco, T. Da Ros, F. Bano, L. Casalis, G. Scoles, M. Prato, *J. Am. Chem. Soc.* **2010**, *132*, 1731.

[55] G. M. Neelgund, A. Oki, *Appl. Catal. B Environ.* **2011**, *110*, 99–107.

[56] M. R. Nabid, Y. Bide, S. J. Tabatabaei Rezaei, *Appl. Catal. A Gen.* **2011**, *406*, 124–132.

[57] M. Sano, A. Kamino, S. Shinkai, *Angew. Chemie - Int. Ed.* **2001**, *40*, 4661–4663.

[58] J. J. Davis, K. S. Coleman, B. R. Azamian, C. B. Bagshaw, M. L. H. Green, *Chem. - A Eur. J.* **2003**, *9*, 3732–3739.

[59] L. Tao, G. Chen, G. Mantovani, S. York, D. M. Haddleton, *Chem. Commun.* **2006**, 4949.

[60] Y. L. Zeng, Y. F. Huang, J. H. Jiang, X. B. Zhang, C. R. Tang, G. L. Shen, R. Q. Yu, *Electrochem. commun.* **2007**, *9*, 185–190.

[61] X. Shi, S. H. Wang, M. Shen, M. E. Antwerp, X. Chen, C. Li, E. J. Petersen, Q. Huang, W. J. Weber, J. R. Baker, *Biomacromolecules* **2009**, 1744–1750.

[62] K. Yang, W. Qin, H. Tang, L. Tan, Q. Xie, M. Ma, Y. Zhang, S. Yao, *J. Biomed. Mater. Res. - Part A* **2011**, *99 A*, 231–239.

[63] Z. Syrgiannis, V. La Parola, C. Hadad, M. Lucío, E. Vázquez, F. Giacalone, M. Prato, *Angew. Chemie - Int. Ed.* **2013**, *52*, 6480–6483.

[64] F. Giacalone, V. Campisciano, C. Calabrese, V. La Parola, Z. Syrgiannis, M. Prato, M. Gruttadauria, *ACS Nano* **2016**, *10*, 4627–4636.

[65] B. Hayati, A. Maleki, F. Najafi, H. Daraei, F. Gharibi, G. McKay, *J. Mol. Liq.* **2016**, *224*, 1032–1040.

[66] L. Valentini, F. Mengoni, I. Armentano, J. M. Kenny, L. Ricco, J. Alongi, M. Trentini, S. Russo, A. Mariani, *J. Appl. Phys.* **2006**, *99*, DOI 10.1063/1.2196147.

[67] J. R. Siqueira, M. H. Abouzar, A. Poghossian, V. Zucolotto, O. N. Oliveira, M. J. Schöning, *Biosens. Bioelectron.* **2009**, *25*, 497–501.

[68] J. R. Siqueira, M. H. Abouzar, M. Bäcker, V. Zucolotto, A. Poghossian, O. N. Oliveira, M. J. Schöning, *Phys. Status Solidi Appl. Mater. Sci.* **2009**, *206*, 462–467.

[69] M. Adeli, S. Beyranvand, R. Kabiri, *Polym. Chem.* **2013**, *4*, 669–674.

[70] V. Vasumathi, D. Pramanik, A. K. Sood, P. K. Maiti, *Soft Matter* **2013**, *9*, 1372–1380.

[71] D. K. Tosh, L. S. Yoo, M. Chinn, K. Hong, S. M. Kilbey, M. O. Barrett, I. P. Fricks, T. K. Harden, Z. G. Gao, K. A. Jacobson, *Bioconjug. Chem.* **2010**, *21*, 372–384.

[72] T. C. Wan, D. K. Tosh, L. Du, E. T. Gizewski, K. A. Jacobson, J. A. Auchampach, *BMC Pharmacol.* **2011**, *11*, 11.

[73] B. Vanhorenbeke, C. Vriamont, F. Pennetreau, M. Devillers, O. Riant, S. Hermans, *Chem. - A Eur. J.* **2013**, *19*, 852–856.

[74] F. Pennetreau, O. Riant, S. Hermans, *Chem. - A Eur. J.* **2014**, *20*, 15009–15012.

[75] A. Desmecht, S. Hermans, O. Riant, *ChemistryOpen* **2017**, *6*, 231–235.

[76] N. Fischer, E. D. Goddard-Borger, R. Greiner, T. M. Klapötke, B. W. Skelton, J. Stierstorfer, *J. Org. Chem.* **2012**, *77*, 1760–1764.

[77] C. Triazole, S. M. Smith, M. J. Greaves, R. Jewell, M. W. D. Perry, M. J. Stocks, J. P. Stonehouse, *Synlett* **2009**, *9*, 1391–1395.

[78] S. Kawasaki, K. Komatsu, F. Okino, H. Touhara, H. Kataura, *Phys. Chem. Chem. Phys.* **2004**, *6*, 1769–1772.

[79] J. L. Bahr, J. Yang, D. V Kosynkin, J. Bronikowski, R. E. Smalley, J. M. Tour, M. J. Bronikowski, *J. Am. Chem. Soc.* **2001**, 6536–6542.

[80] D. Urankar, B. Pinter, A. Pevec, F. De Proft, I. Turel, J. Kosmrlj, *Inorg. Chem.* **2010**, *49*, 4820–4829.

[81] K. J. Kilpin, E. L. Gavey, C. J. Mcadam, C. B. Anderson, S.

Accepted Manuscript

This article is protected by copyright. All rights reserved.

10.1002/chem.201802301

J. Lind, C. C. Keep, K. C. Gordon, J. D. Crowley, *Inorg. Chem.* **2011**, *22*, 6334–6346.

[82] M. Valencia, H. Müller-Bunz, R. A. Gossage, M. Albrecht, *Chem. Commun. (Camb).* **2016**, *52*, 3344–7.

[83] P. Hermange, A. T. Lindhardt, R. H. Taaning, K. Bjerglund, D. Lupp, T. Skrydstrup, *J. Am. Chem. Soc.* **2011**, *133*, 6061–6071.

[84] C. Veryser, S. Van Mileghem, B. Egle, P. Gilles, W. M. De Borggraeve, *React. Chem. Eng.* **2016**, *1*, 142–146.

WILEY-VCH

Accepted Manuscript

This article is protected by copyright. All rights reserved.

10.1002/chem.201802301

WILEY-VCH

Entry for the Table of Contents (Please choose one layout)

Layout 1:

FULL PAPER

We report and compare the covalent and non-covalent immobilization of PAMAM dendrimers on MWNTs. The resulting hybrids were further derivatized, to immobilize homogeneous-*like* iridium complexes or Pd NPs. These were demonstrated efficient for catalytic applications.

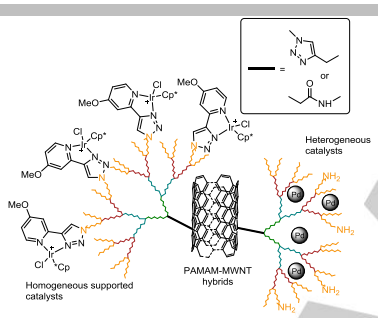

Antonin Desmecht, Timothy Steenhaut, Florence Pennetreau, Sophie Hermans and Olivier Riant**

Page No. – Page No.

Synthesis and Catalytic Applications of Multi-Walled Carbon Nanotube-Polyamidoamine Dendrimer Hybrids

WILEY-VCH Accepted Manuscript

This article is protected by copyright. All rights reserved.